Hindawi
Journal of Chemistry
Volume 2023, Article ID 6678252, 8 pages
https://doi.org/10.1155/2023/6678252

Research Article

A Novel Drug-Drug Salt of Naproxen and Vortioxetine: Synthesis, Characterization, and Solubility Study

Xianrui Zhang and Yuting Gao

College of Food and Pharmaceutical Engineering, Wuzhou University, Wuzhou 543000, China

Correspondence should be addressed to Xianrui Zhang; zhangyang159246@163.com

Received 20 April 2023; Revised 4 July 2023; Accepted 7 July 2023; Published 25 July 2023

Academic Editor: Josefina Pons

Naproxen (NAP) is an aromatic propionic acid nonsteroidal anti-inflammatory drug, and vortioxetine (VOT) is a novel antidepressant drug. In this study, a new 1 : 1 drug-drug salt of NAP and VOT (namely, NAP-VOT) was designed and synthesized by liquid-assisted grinding and slow evaporation. The obtained salt was characterized by single-crystal X-ray diffraction, powder X-ray diffraction (PXRD), and differential scanning calorimetry (DSC). Single-crystal structure showed that NAP-VOT is a molecular salt. The NAP and VOT molecules in the salt were connected by $N\text{-}H^{+}\cdots O$ hydrogen bonds between the carbonyl oxygen of NAP and the piperazine group of VOT. In addition, solubility and dissolution rate experiments were performed in water and pH 6.86 phosphate buffers, and the result suggested that salt formation could increase the solubility and dissolution rate of NAP and VOT in water. Furthermore, this study provides a new research idea to solve the problem of drug-drug combination by achieving drug-drug association at the molecular level.

1. Introduction

Drug-drug cocrystals and salts are an emerging pharmaceutical technology that allows multiple drugs to combine together to improve the efficacy and safety of drugs [1–10]. In recent years, research into drug-drug cocrystal and salts has made great strides and has become a hot topic in the pharmaceutical industry. The advantages of drug cocrystals and salts are that the cocrystal structure can be used to improve drug efficacy and safety, increase drug stability, extend drug shelf life, reduce drug side effects, increase drug bioavailability, reduce drug toxicity, and alter drug efficacy properties and drug intestinal absorption [11–20].

Research has shown that there is an interaction between pain and depression. Chronic pain often triggers depression, and mental depression can exacerbate physical pain, so drug combinations between depression and painkillers have become routine [21, 22]. However, drug combinations are a physical mix and there is no guarantee of physical and chemical compatibility between the two APIs. This paper is the first attempt to achieve a combination between antidepressants and anti-inflammatory and analgesic drugs at the molecular level. Compared to fixed-dose combinations, drug-drug cocrystallization has greater advantages. It avoids the stability and chemical incompatibility problems between drug molecules and is more conducive to drug absorption.

Naproxen is a commonly used aromatic propionic acid nonsteroidal anti-inflammatory drug that exerts anti-inflammatory and analgesic effects by inhibiting the synthesis of prostaglandins [23–26]. Vortioxetine (VOT) is a novel antidepressant that is not only effective in improving the symptoms of depressed patients, but also in improving the mood of depressed patients, reducing anxiety, and improving sleep quality [27–29]. In the present work, a novel drug-drug salt comprised of NAP and VOT (namely NAP-VOT) with a 1 : 1 stoichiometric ratio was synthesized and characterized by single-crystal X-ray diffraction data (SCXRD), powder X-ray diffraction (PXRD), and differential scanning calorimeter (DSC) measurements. In addition, the solubility and powder dissolution rate of the NAP-VOT were compared with that of the parent drug NAP and VOT.

The molecular structures of NAP and VOT are displayed in Scheme 1.

2. Experimental Section

2.1. Instrumentations and Materials. All chemicals and reagents were obtained from a variety of business sources and utilized without further purification. The powder X-ray diffraction (PXRD) of NAP, VOT, and NAP-VOT salt were performed using a Bruker corporation D8 ADVANCE diffractometer with a Cu-Kα radiation tube ($\lambda = 1.5418$ Å) at 40 mA and 40 kV. Differential scanning calorimetry (DSC) measurements were performed on a Mettler–Toledo analyzer at a heating rate of 10°C/min in a nitrogen environment. On a Bruker Apex II CCD diffractometer operating at 50 kV and 30 mA, single-crystal X-ray diffraction measurements of the NAP-VOT was recorded using Mo Kα radiation ($\lambda = 0.71073$ Å). The SHELXS program was used to solve the crystal structure, which was then refined with the SHELXL program [30]. The NAP-VOT salt was analyzed and produced on the basis of its single-crystal data using CrystalExplorer 3.1 software. Tables 1 and 2 show the crystal structure parameters as well as hydrogen bond distances and angles.

2.2. Preparation of NAP-VOT. NAP-VOT salt was synthesized using a slow evaporation method. NAP (10 mg, 43.4 mmol) and VOT (13 mg, 43.4 mmol) solutions were prepared in a 1 : 1 equimolar ratio using a mixture of solvents (5 mL, acetonitrile: water, *v*/*v* 80 : 20%). The solutions were stirred at 50°C for 1 hour and left to evaporate slowly at room temperature. After 7–10 days, colorless needle crystals were obtained. Yield: 7.2 mg (31%). NAP-VOT salt was also prepared by the acetonitrile-assisted grinding method.

2.3. High-Performance Liquid Chromatography (HPLC) Assay. The concentration of NAP and VOT was determined by an Agilent 1260 Infinity II HPLC system. NAP and VOT were separated by an EC-C18 column (150 mm × 3.0 mm and 2.7 μm particle size). Mobile phase consisting of 60 : 40 (v/v) acetonitrile and potassium phosphate (pH 2.50, 0.01 M) was run at 0.6 mL/min. The column temperature was kept at 35°C and both NAP and VOT were detected at 226 nm.

2.4. Solubility and Powder Dissolution Studies. Solubility and powder dissolution tests were carried out in a round-bottomed flask containing water and pH 6.86 phosphate buffer medium at 37 ± 0.5°C. Excess sample was added to 25 mL mother liquor in a round bottom flask and stirred magnetically for 24 h. Then, the suspension was taken and filtered through a 0.22 μm membrane and the concentration of the filtrate was determined and analyzed by HPLC ($n = 3$). Residual samples were also collected for PXRD and DSC testing, the aim of which was to determine the stability of the residual samples. Powder dissolution experiments were similar to the solubility test, the difference being that the samples were taken at a fixed point in time while an equal amount of fresh mother liquor is added to keep the volume of the solution constant.

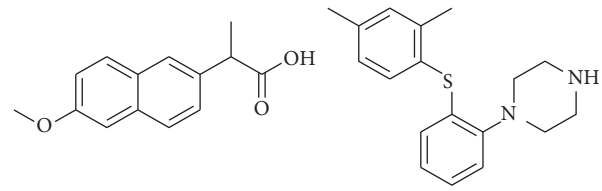

Scheme 1: Molecular structures of NAP and VOT.

Table 1: Crystallographic parameters of NAP-VOT.

	NAP-VOT
Chemical formula	$C_{18}H_{23}N_2S$, $C_{14}H_{13}O_3$
Formula sum	$C_{32}H_{36}N_2O_3S$
Formula weight	528.69
Crystal system	Monoclinic
Space group	*P*121/*c*1
a (Å)	22.6926 (14)
b (Å)	5.7544 (5)
c (Å)	22.7571 (13)
α (°)	90
β (°)	106.627 (6)
γ (°)	90
Z	4
V (Å^3)	2847.4 (4)
D_{calc} (g cm^{-3})	1.233
M (mm^{-1})	0.149
R_1 [$I > 2\sigma$ (*I*)]	0.1158
wR_2 (all data, F^2)	0.2143
GOF	1.142
Largest diff. peak and hole (e·Å^{-3})	0.468/−0.359
CCDC	2234586

Table 2: Hydrogen bond distances (Å) and angles (°) of NAP-VOT.

H-bond	d (D–H)	d (H···A)	d (D···A)	∠ (DHA)
N1-H1C$^+$···O2^{i}	0.91	1.88	2.742 (5)	154
N1-H1D$^+$···O1^{ii}	1.03	1.68	2.700 (3)	171

Symmetry codes: (i) *x*, −*y* + 3/2, *z* + 1/2; (ii) −x, *y* + 3/2, −z + 1/2.

3. Results and Discussion

3.1. Crystal Structure Analyses. The crystal structure of NAP drug (CCDC reference: 1130671 [31]) showed that adjacent NAP molecules were associated through strong O-H···O (O2-H14···O3, 1.63 Å, 162°) hydrogen bonds in a one-dimensional wavy linear structure (Figure 1). The crystal structure of VOT drug (CCDC reference: 1408949 [32]) revealed that VOT molecules formed a parallel displaced manner through $\pi\cdots\pi$ interactions (Figure 2). In NAP-VOT salt, these abovementioned hydrogen bonds and $\pi\cdots\pi$ interactions belonging to NAP and VOT single crystals were substituted by stronger ionic variant carboxylate···piperazine salt heterosynthons. NAP-VOT salt crystallized in the monoclinic crystal system with the *P*121/*c*1 space group and comprised one NAP anion and one VOT

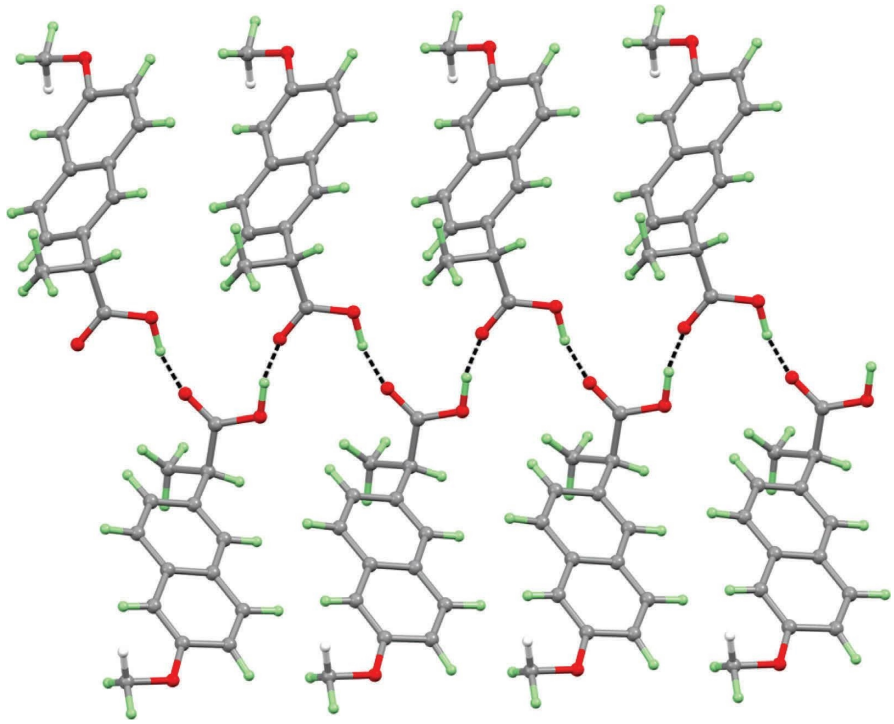

Figure 1: 1D chains of NAP molecules connected through O-H···O hydrogen bonds.

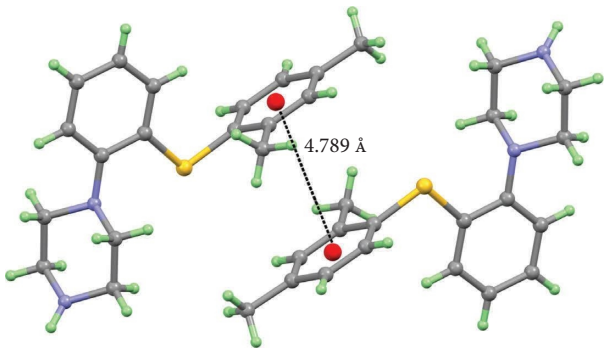

Figure 2: The VOT molecules formed a parallel displaced manner through $\pi\cdots\pi$ interactions with centroid-centroid distances of 4.789 Å.

cation in the asymmetric unit. Two NAP anions and two VOT cations formed a R_4^4 (12) tetramer through N1-H1C$^+$···O2 (1.88 Å, 154°) and N1-H1D$^+$···O1 (1.68 Å, 171°) hydrogen bonds, and these R_4^4 (12) tetramer were further bridged through C-H···π interactions (Figure 3).

3.2. Hirshfeld Surface Analyses. Hirshfeld surface analysis provides a visual insight into the weak force interactions between molecules [33, 34]. In order to compare the change in molecular weak forces after salt formation, the Hirshfeld surface analyses of NAP, VOT, and NAP-VOT were generated, and the Hirshfeld surfaces are shown in Figure 4. As can be seen from Figure 4, the H···H weak interaction contribution values in NAP, VOT, and NAP-VOT account for 44.8%, 74.2%, and 58.5%, respectively. It is clear that the H···H weakly interacting contribution values are dominant in the corresponding groups, where the contribution of H···H weakly interacting NAP is smaller than that of VOT. Currently, the H···H weak interaction contribution values of NAP-VOT are between NAP and VOT, indicating the NAP-VOT are structurally denser than NAP and looser VOT, which provide an opportunity to regulate the NAP and VOT solubility by creating favourable conditions. In addition, the intermolecular O---H hydrogen bonding interactions in NAP-VOT have a combined polar contact of 14.1%, which is better than that of pure VOT molecules (0%). The enhanced polar weak interaction provides more polar bonding sites for the solvation effect, which might enhance the solubility of NAP-VOT.

3.3. PXRD Analyses. The PXRD patterns for NAP, VOT, and NAP-VOT are presented in Figure 5. NAP-VOT displayed major diffraction peaks at 4.04°, 8.04°, 9.66°, 12.52°, 12.96°, 15.48°, 15.9°, 17.3°, 18.18°, 19.62°, 21.22°, 22.36°, 23.44°, 24.96°, 25.62°, and 28.6°. Diffraction peaks at 2θ values of 6.44°, 12.48°, 13.16°, 16.64°, 17.82°, 18.82°, 20.16°, 22.4°, 23.54°, 27.2°, 27.64°, 28.38°, 29.7°, and 31.16° in NAP, and 11.06°, 12.36°, 14.32°, 16.86°, 17.4°, 18.64°, 19.04°, 22.48°, 24.38°, and 25.66° in VOT. The diffractogram of NAP-VOT was distinguishable from NAP and VOT, indicating the formation of a new crystalline phase. In addition, the experimental PXRD pattern of NAP-VOT was in good agreement with the calculated profile, suggesting the high purity of the powder sample.

3.4. Thermal Analyses. Thermal behaviours of NAP, VOT, and NAP-VOT are tested using differential scanning calorimetry (DSC), and thermograms are presented in

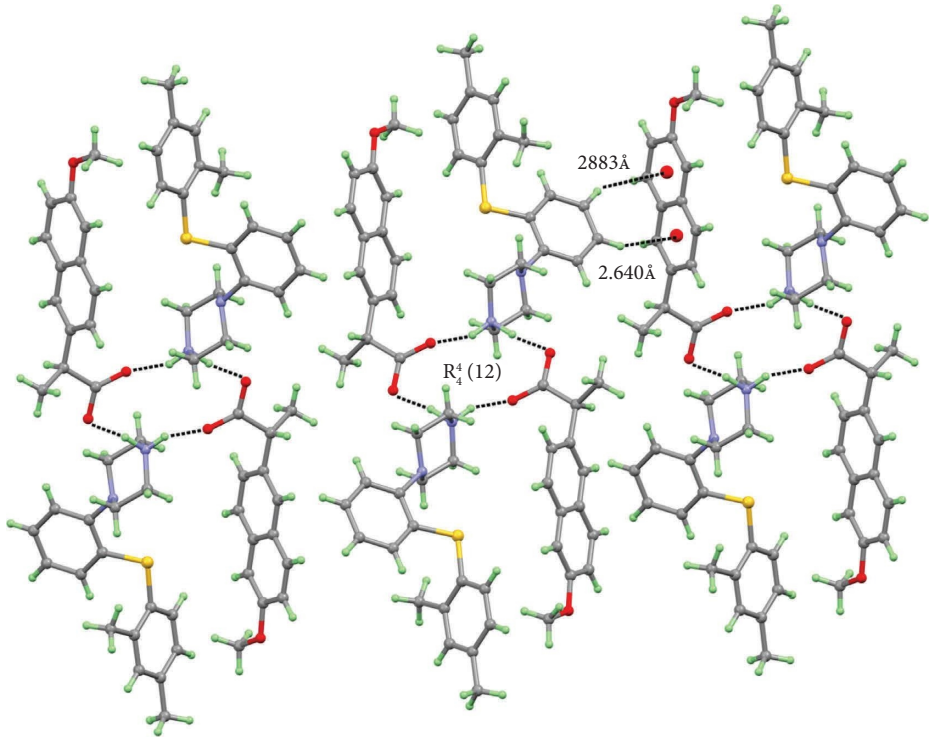

Figure 3: Two NAP anions and two VOT cations formed a R_4^4 (12) tetramer through N1-H1C$^+$···O2 and N1-H1D$^+$···O1 hydrogen bonds.

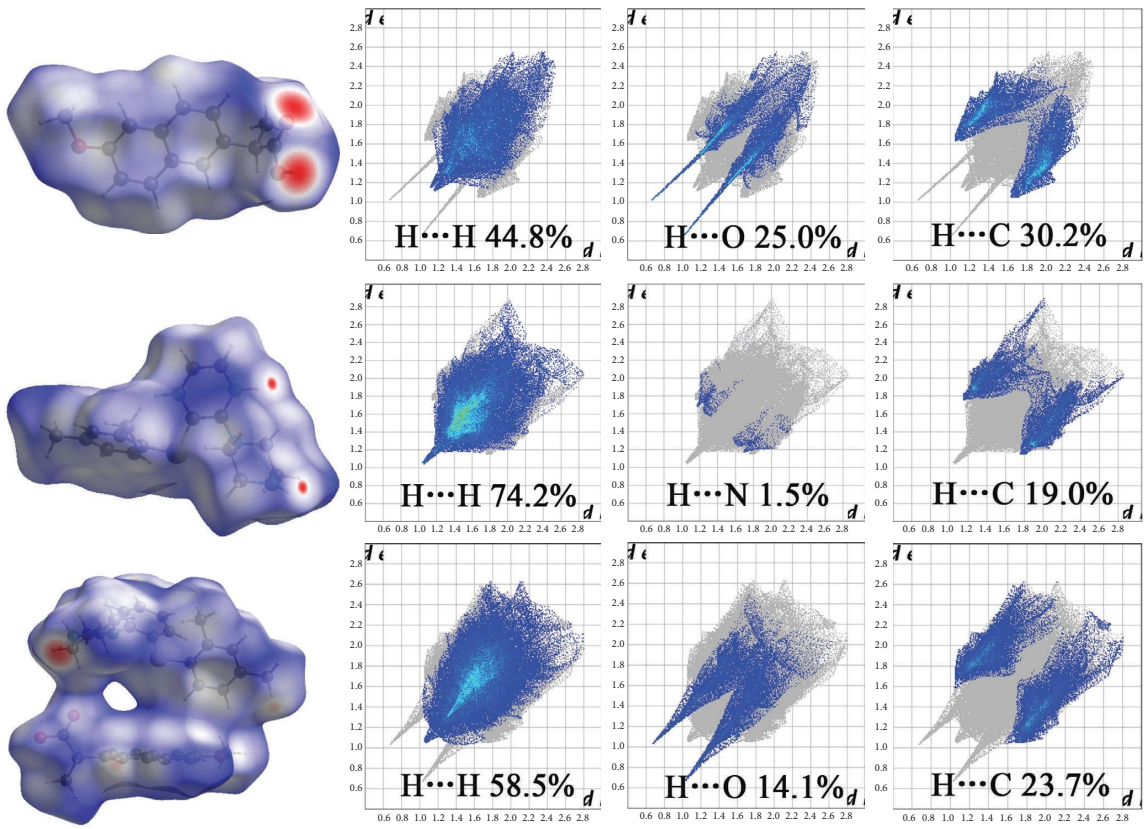

Figure 4: Hirshfeld surface for NAP, VOT, and NAP-VOT salt mapped with d_{norm}.

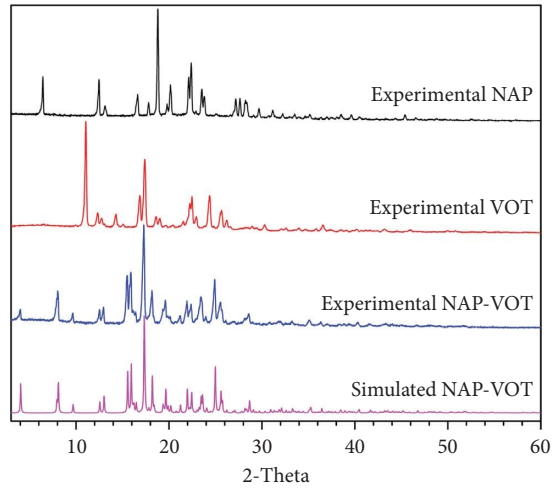

Figure 5: PXRD pattern of experimental NAP, experimental VOT, experimental NAP-VOT, and simulated NAP-VOT.

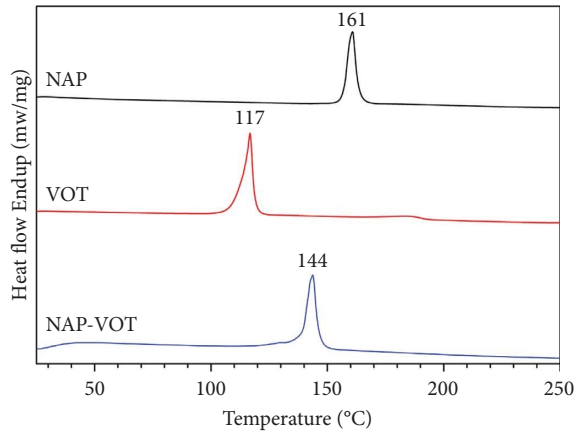

Figure 6: The DSC thermograms of NAP, VOT, and NAP-VOT.

Table 3: Measured solubility values of NAP, VOT, and NAP-VOT in water and pH 6.86 buffer solutions at 37°C.

Medium	Compound	Concentration (mmol/L)	Residue obtained in solubility experiment after 24 h
Water	NAP	21.44×10^{-2}	Stable
	VOT	15.00×10^{-2}	Stable
	NAP-VOT	27.69×10^{-2}	Stable
pH 6.86	NAP	8.53	Stable
	VOT	17.57×10^{-2}	Unstable
	NAP-VOT	48.34×10^{-2}	Stable

Figure 6. Crystalline NAP, VOT, and NAP-VOT exhibited single-endothermic peak at 161°C, 117°C, and 144°C, respectively. The endothermic peak of NAP-VOT was between NAP and VOT, indicating the formation of a new solid form.

3.5. Solubility and Dissolution Studies. The solubility of NAP, VOT, and NAP-VOT in pure water and pH 6.86 buffer solution are shown in Table 3. The solubility order was NAP-VOT > NAP > VOT in water and NAP > NAP-VOT > VOT in pH 6.86 buffer solution. The NAP-VOT salt showed better

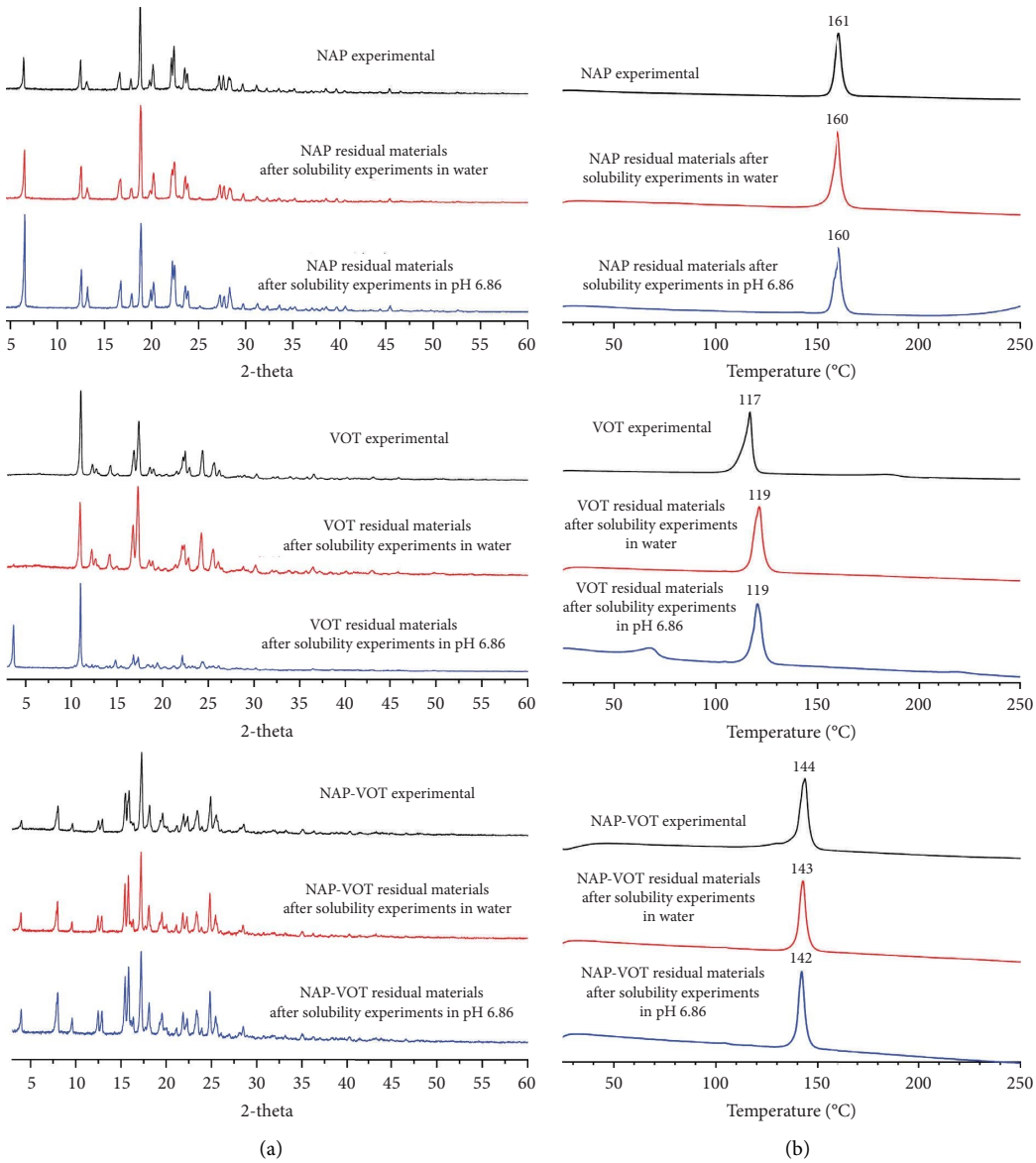

Figure 7: Comparison of (a) PXRD and (b) DSC curves of experimental and residual materials of NAP, VOT, and NAP-VOT in water and pH 6.86 buffer solutions.

solubility in water when compared to NAP and VOT, while the solubility of NAP-VOT at pH 6.86 phosphate buffers was in between that of NAP and VOT. The formation of the remaining materials after solubility studies was tested through PXRD and DSC, and the result of PXRD and DSC is shown in Figure 7. The remaining solids showed that NAP and NAP-VOT were stable in water and pH 6.86 buffer solutions, but VOT was unstable in pH 6.86.

The powder dissolution profiles of NAP-VOT were evaluated in water and pH 6.86 phosphate buffers, and the results are shown in Figure 8. The result showed that the dissolution profile of NAP-VOT in pH 6.86 was lower than

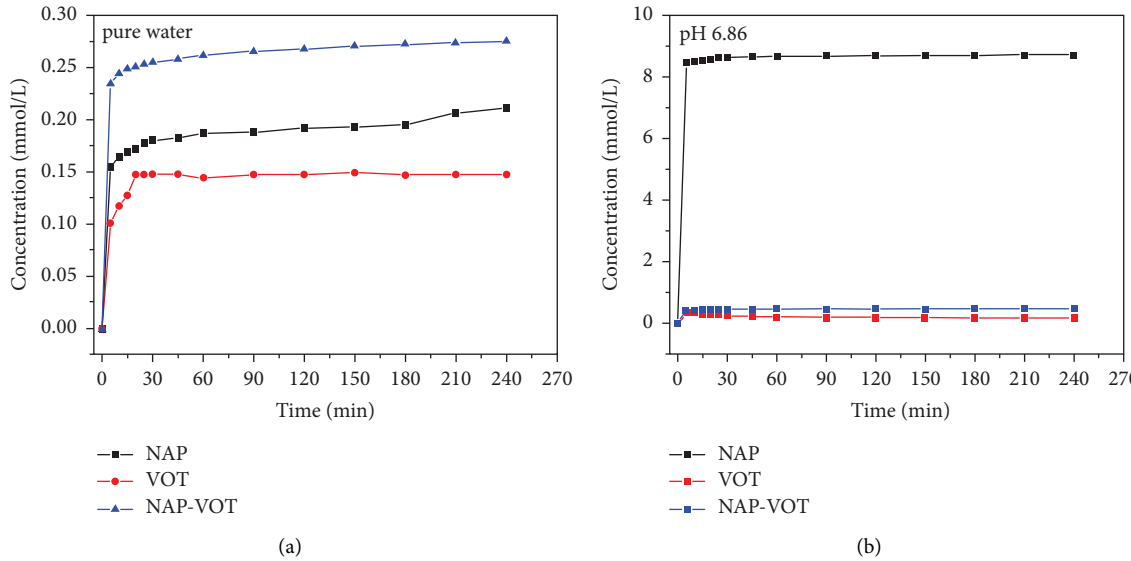

Figure 8: The powder dissolution profiles of NAP, VOT, and NAP-VOT.

NAP but better than VOT. On the other hand, the dissolution rate of NAP-VOT in water is superior to that of NAP and VOT.

4. Conclusions

In conclusion, a novel drug-drug salt comprised of NAP and VOT (NAP-VOT) with a 1 : 1 stoichiometric ratio was synthesized to solve the absorption problem when coadministering drugs and to truly achieve drug combination at the molecular level. The NAP and VOT molecules in the salt were connected by N-$H^{+}\cdots$O hydrogen bonds between the carbonyl oxygen of NAP and the piperazine group of VOT. In addition, the physicochemical properties, solubility, and dissolution rates of the salt were systematically investigated. As expected, the solubility and dissolution rate of the NAP-VOT salt significantly increased in comparison to NAP and VOT in water. Furthermore, this study is an important guide to address the problem of poor adherence to medication in drug combinations.

Data Availability

CCDC 2234586 contains the supplementary crystallographic data for this paper. These data can be obtained free of charge from The Cambridge Crystallographic Data Centre via https://www.ccdc.cam.ac.uk/structures.

Conflicts of Interest

The authors declare that they have no conflicts of interest.

Authors' Contributions

The manuscript was written and analyzed through contributions of all authors. All authors conceptualized and designed the study. Material preparation and experimental study were performed by Xianrui Zhang and Yuting Gao. The data analysis and software calculation were performed by Xianrui Zhang. The funding support and first draft of the manuscript were written by Xianrui Zhang and all authors commented on the previous version of the manuscript. All authors read and approved the final manuscript.

Acknowledgments

This work was supported by the Guangxi Science and Technology Base and Talent Project (grant no. GUIKE AD20159051); Wuzhou University Foundation (grant no. 2020B006), and Innovation and Entrepreneurship Training Program for College Students (grant no. 202211354012).

References

[1] L. Liu, D. Zou, Y. Zhang et al., "Assembly of three pharmaceutical salts/cocrystals of tetrahydroberberine with sulfophenyl acids: impriving the properties by formation of charge-assisted hydrogen bonds," *New Journal of Chemistry*, vol. 43, no. 12, pp. 4886–4894, 2019.

[2] S. M. Berge, L. D. Bighley, and D. C. Monkhouse, "Pharmaceutical salts," *Journal of Pharmaceutical Sciences*, vol. 66, no. 1, pp. 1–19, 1977.

[3] P. Deka, D. Gogoi, K. Althubeiti, D. R. Rao, and R. Thakuria, "Mechanosynthesis, characterization, and physicochemical property investigation of a favipiravir cocrystal with theophylline and GRAS coformers," *Crystal Growth & Design*, vol. 21, no. 8, pp. 4417–4425, 2021.

[4] A. T. Serajuddin, "Salt formation to improve drug solubility," *Advanced Drug Delivery Reviews*, vol. 59, no. 7, pp. 603–616, 2007.

[5] B. Park, W. Yoon, J. Yun, E. Ban, H. Yun, and A. Kim, "Emodin-nicotinamide (1:2) cocrystal identified by thermal screening to improve emodin solubility," *International Journal of Pharmaceutics*, vol. 557, pp. 26–35, 2019.

[6] S. K. Nechipadappu and D. R. Truvedi, "Pharmaceutical salts of ethionamide with GRAS counter ion donors to enhance the

solubility," *European Journal of Pharmaceutical Sciences*, vol. 96, pp. 578–589, 2017.

[7] L. Bofill, R. Barbas, D. de Sande et al., "A novel, extremely bioavailable cocrystal of pterostilbene," *Crystal Growth & Design*, vol. 21, no. 4, pp. 2315–2323, 2021.

[8] J. Li, X. Hao, C. Wang et al., "Improving the solubility, dissolution, and bioavailability of metronidazole via cocrystallization with ethyl gallate," *Pharmaceutics*, vol. 13, no. 4, p. 546, 2021.

[9] Y. Liu, F. Yang, X. Zhao, S. Wang, Q. Yang, and X. Zhang, "Crystal structure, solubility, and pharmacokinetic study on a hesperetin cocrystal with piperine as coformer," *Pharmaceutics*, vol. 14, no. 1, 2022.

[10] L. Gao, W. Y. Zheng, W. L. Yang, and X. R. Zhang, "Drug-drug salt forms of vortioxetine with mefenamic acid and tolfenamic acid," *Journal of Molecular Structure*, vol. 1268, 2022.

[11] S. F. He, X. R. Zhang, S. Zhang, S. Guan, J. Li, and S. Li, "An investigation into vortioxetine salts: crystal structure, thermal stability, and solubilization," *Journal of Pharmaceutical Sciences*, vol. 105, no. 7, pp. 2123–2128, 2016.

[12] Z. Rahman, C. Agarabi, A. S. Zidan, S. R. Khan, and M. A. Khan, "Physico-mechanical and stability evaluation of carbamazepine cocrystal with nicotinamide," *AAPS PharmSciTech*, vol. 12, pp. 693–704, 2011.

[13] J. Wang, X. L. Dai, T. B. Lu, and J. M. Chen, "Temozolimide-hesperetin drug-drug cocrystal with optimized performance in stability, dissolution, and tabletability," *Crystal Growth & Design*, vol. 21, no. 2, pp. 838–846, 2021.

[14] J. Li, L. Y. Li, S. F. He, S. Li, C. Z. Dong, and L. Zhang, "Crystal structures, X-ray photoelectron spectroscopy, thermodynamic stabilities, and improved solubilities of 2-hydrochloride salts of vortioxetine," *Journal of Pharmaceutical Sciences*, vol. 106, no. 4, pp. 1069–1074, 2017.

[15] P. S. Carvalho, L. F. Diniz, J. C. Tenorio et al., "Pharmaceutical paroxetine-based organic salts of carboxylic acids with optimized properties: the identification and characterization of potential novel API solid forms," *CrystEngComm*, vol. 21, no. 24, pp. 3668–3678, 2019.

[16] M. K. Gautam, M. Besan, D. Pandit, S. Mandal, and R. Chadha, "Cocrystal of 5-fluorouracil: characterization and evaluation of biopharmaceutical paprameters," *AAPS PharmSciTech*, vol. 20, pp. 1–17, 2019.

[17] B. C. D. Owoyemi, C. C. da Silva, L. F. Diniz, M. S. Souza, J. Ellena, and R. L. Carneiro, "Fluconazolium oxalate: synthesis and structural characterization of a highly soluble crystalline form," *CrystEngComm*, vol. 21, no. 7, pp. 1114–1121, 2019.

[18] P. Sanphui, S. Tothadi, S. Ganguly, and G. R. Desiraju, "Salt and cocrystals of sildenafil with dicarboxylic acids: solubility and pharmacokinetic advantage of the glutarate salt," *Molecular Pharmaceutics*, vol. 10, no. 12, pp. 4687–4697, 2013.

[19] M. R. Arabiani, A. Lodagekar, B. Yadav et al., "Mechanochemical synthesis of brexpiprazole cocrystals to improve its pharmaceutical attributes," *CrystEngComm*, vol. 21, no. 5, pp. 800–806, 2019.

[20] H. Afzal, N. Abbas, A. Hussain, S. Latif, K. Fatima, and M. S. Arshad, "Physicomechanical stability, and pharmacokinetic evaluation of aceclofenac dimethyl urea cocrystals," *AAPS PharmSciTech*, vol. 22, pp. 1–13, 2021.

[21] J. F. Cryan, M. E. Page, and I. Lucki, "Differential behavioral effects of the antidepressants reboxetine, fluoxetine, and moclobemide in a modified forced swim test following chronic treatment," *Psychopharmacology*, vol. 182, pp. 335–344, 2005.

[22] A. D. Holzberg, M. E. Robinson, M. E. Geisser, and H. A. Gremillion, "The effects of depression and chronic pain on psychosocial and physical functioning," *The Clinical Journal of Pain*, vol. 12, no. 2, pp. 118–125, 1996.

[23] P. J. Harrington and E. Lodewijk, "Large-scale synthetic process for (S)-naproxen by syntex," *Organic Process Research & Development*, vol. 1, pp. 72–76, 1997.

[24] ADAPT Research Group, "Naproxen and celecoxib do not prevent AD in early results from a randomized controlled trial," *Neurology*, vol. 68, no. 21, pp. 1800–1808, 2007.

[25] N. M. Davies and K. E. Anderson, "Clinical pharmacokinetics of naproxen," *Clinical Pharmacokinetics*, vol. 32, pp. 268–293, 1997.

[26] P. A. Todd and S. P. Clissold, "Drugs," *Drugs*, vol. 40, no. 1, pp. 91–137, 1990.

[27] G. Chen, A. M. Højer, J. Areberg, and G. Nomikos, "Vortioxetine: clinical pharmacokinetics and drug interactions," *Clinical Pharmacokinetics*, vol. 57, pp. 673–686, 2018.

[28] G. Chen, W. Zhang, and M. Serenko, "Lack of effect of multiple doses of vortioxetine on the pharmacokinetics and pharmacodynamics of aspirin and warfarin," *The Journal of Clinical Pharmacology*, vol. 55, no. 6, pp. 671–679, 2015.

[29] J. Areberg, K. B. Petersen, G. Chen, and H. Naik, "Population pharmacokinetic meta-analysis of vortioxetine in healthy individuals," *Basic and Clinical Pharmacology and Toxicology*, vol. 115, no. 6, pp. 552–559, 2014.

[30] G. M. Sheldrick, *Shelxl-97*, University of Gottingen, Germany, 1997.

[31] K. Ravikumar, S. S. Rajan, V. Pattabhi, and E. J. Gabe, "Structure of naproxen, C14H14O3," *Acta Crystallographica Section C Crystal Structure Communications*, vol. 21, no. 2, pp. 280–282, 1985.

[32] X. B. Zhou, J. M. Gu, M. Y. Sun, X. R. Hu, and S. X. Wu, "Crystal structures of vortioxetine and its methanol monosolvate," *Acta Crystallographica Section E: Crystallographic Communications*, vol. 71, no. 8, pp. 883–885, 2015.

[33] J. J. Mckinnon, D. Jayatilaka, and M. A. Spackman, "Towards quantitative analysis of intermolecular interactions with Hirshfeld surfaces," *Chemical Communications*, vol. 37, pp. 3814–3816, 2007.

[34] M. A. Spackman and D. Jayatilaka, "Hirshfeld surface analysis," *CrystEngComm*, vol. 11, no. 1, pp. 19–32, 2009.